Intermodality, Retrospective Image Registration in the Thorax

Jeffrey N. Yu, Frederic H. Fahey, Howard D. Gage, Cathy G. Eades, Beth A. Harkness, Charles A. Pelizzari and John W. Keyes Jr.

PET Center, Bowman Gray School of Medicine of Wake Forest University, Winston-Salem, North Carolina; and the Department of Radiation Oncology, University of Chicago, Chicago, Illinois

The purpose of this study was to develop an accurate, retrospectively applicable procedure for registering thoracic studies from different modalities in a short amount of time and with minimal operator intervention. **Methods:** CT and PET studies were acquired from six patients. The pleural surfaces in both image sets were determined by segmenting based on 50% of the maximum soft-tissue value in the study. These surfaces were converted into three-dimensional volumes and used to register the CT and PET studies in three dimensions using a sum of a least squares fitting approach. The registered PET study was then displayed in a hot metal scale overlayed on top of the gray scale CT study. The accuracy of the fit was evaluated through a phantom study and preliminary clinical evaluation. **Results:** A phantom study was performed to determine the limits of this technique. The accuracy was determined to be less than 2.3 mm in the x and y direction and 3 mm in the z direction. Preliminary clinical evaluation was also performed with encouraging results. **Conclusion:** This technique accurately registers PET and CT images of the thorax, retrospectively, without the need for external fiducial markers or other a priori action.

Key Words: positron emission tomography; computed tomography; image registration; thorax

J Nucl Med 1995; 36:2333–2338

T here has been much interest in the use of PET to image the thorax. PET has already been established as an accurate method for determining the viability of myocardial tissue (*1*). Additionally, PET has been shown to be quite sensitive in the detection of lung carcinoma (*2*). PET presents functional information but very little in the way of anatomical information. CT is superb for demonstrating fine anatomical detail but does not provide information on the functional aspects of the tissue. We sought to combine the strengths of these two modalities into a single, combined display format for imaging the thorax. This requires the registration of the image data from the two modalities. In addition, the ability to apply such a registration method

retrospectively (that is requiring no preparation prior to acquisition such as the placement of fiducial markers) was considered imperative for the method to be of practical clinical value.

Much of the work in registration involving PET has been in the brain (*3–5*). The brain registration method described by Pelizzari et al. has been shown to be accurate and can be applied retrospectively (*6–8*). In the thorax, Bettinardi (*9*) and Bacharach (*10*) have described methods to register PET emission and transmission images to ensure accurate attenuation correction. Kramer et al. have registered CT and SPECT studies in the abdomen for the evaluation of monoclonal antibody studies (*11*). Wahl et al. have "fused" PET and CT or MR images in the thorax using a combination of external fiducial markers and internal anatomical landmarks with a reported accuracy of 5–6 mm and a processing time of less than 2 hr (*12*).

Techniques based on external fiducial markers require that candidates for the registration procedure be known in advance, as fiducials must be placed on the patient prior to both of the scans and be maintained in the same position until both studies are completed. This precludes the registration of studies performed without fiducial markings and limits the application of registration to those known to need registration a priori. Additionally, fiducials attached to the skin can be affected by movement of the skin relative to the internal structures. This effect is especially likely in the obese patient in which the fat pannus allows marked movement of the skin relative to the thoracic cage. Wahl et al. note the advantage of a technique which does not require fiducial markers and which can be applied in retrospect (*12*).

Our goal was to develop a clinically applicable registration technique which could be used in retrospect without requiring prior placement of fiducial markers. The success of the surface-fitting algorithm for registration of brain studies (*6*) led us to seek ways to apply this algorithm in the thorax. For these reasons, we sought to identify a structure in the thorax that would be suitable for use with the surface-fitting algorithm. The criteria for selection were that it exhibit easily discernable surfaces in both PET and CT, that its orientation with respect to structures of interest (primary tumor and lymph nodes) be fixed and that it be

asymmetric enough to allow for an accurate registration. It was determined that the pleural surfaces of the lungs best met these criteria.

We have developed a segmenting methodology to utilize the surface-fitting algorithm allowing for accurate registration of these two modalities retrospectively and have evaluated its accuracy through a phantom study. A limited clinical evaluation of the technique was performed to demonstrate its clinical potential.

METHODS

CT and PET 2-fluoro-2-deoxy-d-glucose (FDG) studies of six patients, obtained during a clinical study of the efficacy of PET scanning in lung cancer staging, provided the image data for this project. CT images of the chest were acquired as 512 × 512 × 12-bit images with approximately 30 slices per study and a center-to-center slice spacing of 10 mm. These images were electronically transferred from the CT host computer to the Sun Sparc 2 workstation in the PET center. If the CT data were not online, they were uploaded from the optical archive prior to transfer. PET images were acquired as 128 × 128 × 16-bit images with 124 slices spaced 3.13 mm apart. As part of the PET scanning protocol, two different types of images are acquired: a transmission study (used for attenuation correction) and an emission study showing tracer uptake. The CT and PET images were converted to a common format (256 × 256 × 16-bit) by reducing the 512 × 512 CT images through pixel averaging and by expanding the 128 × 128 PET images through pixel replication. The full-bit depths of both images were retained. All image processing was performed on a Sun Sparc 2 (Sun Microsystems, Inc., Mountain View, CA).

The pleural surfaces of the lungs were used to register the two modalities. For the PET study, the transmission image set was used to define the pleural surfaces. We have previously shown that the thoracic transmission scan is adequately aligned with the emission scan when using the laser alignment system built into our scanner (13). Both the PET and CT data were automatically segmented by thresholding using a program that was developed in-house. The CT data were thresholded at a fixed value for all patients which represented approximately 50% of the soft-tissue value. The PET transmission scan was thresholded at 50% of the maximum soft tissue value for each individual study. As will be discussed later, the use of these thresholds was validated through the phantom study. The maximum soft-tissue value was determined by drawing a region of interest (ROI) lateral to the lung in the PET transmission scan and determining the maximum value in all slices of the study within this ROI.

The pleural surfaces of the chest wall were segmented from the most anterior to the most posterior points for each lung as shown in Figure 1. This avoided the mediastinum, which previous experience demonstrated to be too variable for accurate registration (13). The pleural margins are very reliable for surface definition because normal, quiet respiration is primarily diaphragmatic and involves minimal motion of the rib cage. The algorithm used for image registration was the surface-fitting algorithm developed by Pelizzari et al. (6). This algorithm models the contours from one of the image sets as a surface (the "head") and the contours of the second image set as a series of points (the "hat"). It then determines the optimum transformation as that which minimizes the mean squared deviation between the points of the hat and the surfaces of the head. The pixel size and center-to-center slice spacing information for the CT and PET images were entered into

the surface-fitting program. The pleural surfaces from the two image sets (CT and PET) were converted into a format acceptable by the surface-fitting algorithm, with the CT image surfaces being converted into contours (the head file) and the PET image surfaces being converted into a set of points (the hat file). The surface-fitting program was allowed to vary the translations and rotations in all three dimensions. Scaling was set by the pixel sizes of each modality entered into the algorithm. The transformation required to register the two image sets was then used to reslice the PET emission and transmission image sets to match the CT image set.

Finally, the resliced PET emission image set was merged with the CT image set to produce a combined display using two color scales. In this merged image, the CT information is displayed in gray scale and the PET information is displayed in a hot metal scale. This display technique was also used to overlay sliced transmission images on the CT images to assist in verifying the registration process.

To evaluate the accuracy of the CT-PET registration in the thorax, a phantom study was performed. The Alderson thoracic phantom was used to validate the accuracy of this method of image registration and to determine the optimum threshold to use on the PET transmission scans to segment the pleural contours. All thoracic compartments of the phantom except the lungs (e.g., the thyroid, the cardiac chambers and the thoracic soft tissue compartments) were filled with water. The two lung compartments were filled with air. Nine markers were then placed at various locations on the phantom and used to provide an independent and objective measure of the goodness of registration. The locations of the nine markers were chosen such that they covered the entire area of interest (the entire extent of the lungs in the phantom), and no two markers were in the same PET transverse plane. These markers consisted of syringe caps that were filed until they could be snapped onto nonmetallic electrocardiogram (EKG) leads. The EKG leads were affixed to the phantom at the selected locations, and then the syringe caps were snapped into place. These plain markers were easily seen on CT but were not visible on the PET transmission scan. For the PET transmission scans, small lead markers (less than 4 mm in diameter) were taped to the end of syringe caps. The lead markers were not used for the CT scan since they would have led to substantial streak artifacts and the syringe caps themselves were easily visible.

A helical CT and four separate PET transmission scans were acquired of the marked phantom. The four PET transmission scans were acquired in four different orientations, i.e., the phantom was translated and rotated between each of the four acquisitions. The CT scan was acquired on a CT scanner and reconstructed into a 512 × 512 matrix and then reduced by pixel averaging to a 256 × 256 matrix (1.406 mm pixel size) with a 2.5 mm center-to-center slice spacing. The PET transmission scans were acquired with the PET scanner and reconstructed exactly as described for the clinical studies.

The locations of the nine markers in Cartesian coordinates were then determined for the five studies. For the CT study, the distal aspect of each marker was determined visually from a three-view display that provided transverse, sagittal and coronal views of the phantom. For the PET transmission scan, the x and y coordinates were determined by finding the centroid of each marker in the transverse image and the z coordinate was determined from the centroid of the marker in the sagittal view.

All five scans were then segmented by a thresholding technique as described with the clinical studies to determine the contours to
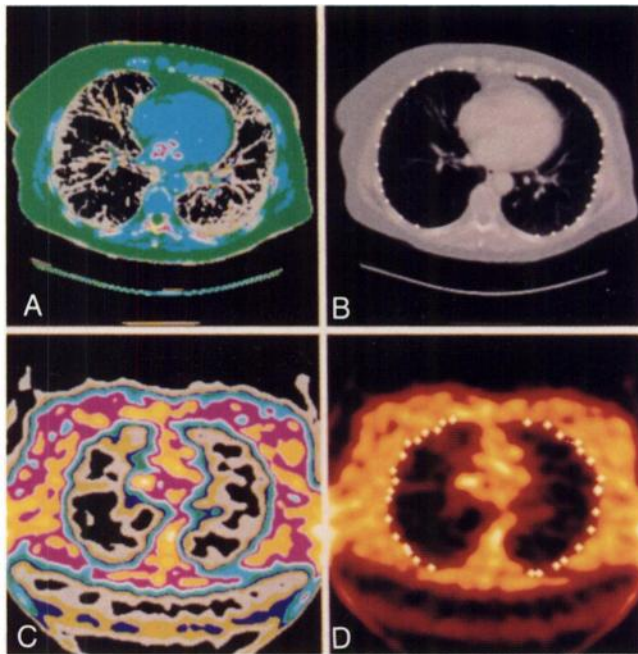
FIGURE 1. Contours used for registration. (A,C) CT and PET transmission scans, respectively, displayed in an isocontour color table. The isocontour images helped us to determine the contours to be used in the registration procedure. The points defining the contours are shown as points overlayed on the images (B,D).

FIGURE 2. Total and z rms deviations along with the average deviation in z as a function of the threshold value. The optimum threshold corresponds to the one that leads to an average z deviation of zero and corresponds to a threshold value of between 0.060 and 0.065 (50–54%).

be used for the registration algorithm. Due to the sharp gradient at the pleural surface boundary on the CT scan, any threshold between 30% and 70% of the soft-tissue value yielded basically the same contour, thus 50% was chosen as the threshold. The four PET transmission scans were each segmented six times with six different thresholds (0.04, 0.05, 0.055, 0.060, 0.065, 0.07). Since the maximum value of these scans was about 0.12, these thresholds represented approximately 33%, 42%, 46%, 50%, 54% and 58% of the maximum value, respectively. The surface-fitting algorithm described for the clinical studies was then used to register each of the four PET transmission studies to the CT study using the CT scan as the head and the PET transmission studies as the hat.

For each of the four cases, the parameters file generated by the registration software was used to determine the transformation matrix that, wh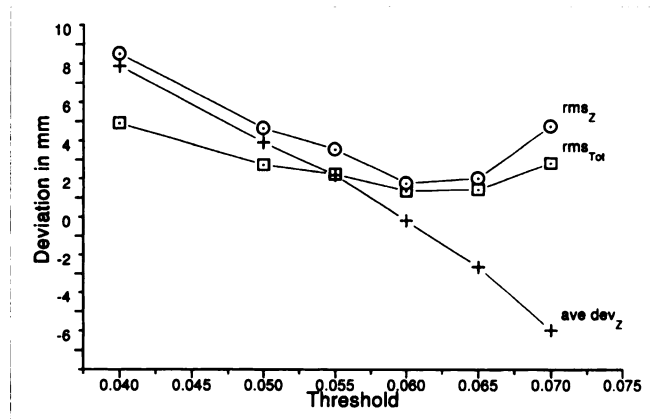en applied to the hat file, would register it with the head file. This transformation matrix was then applied to a matrix consisting of the locations of the nine markers to transform them to their locations in the CT scan. The root mean square (rms) deviation of the registered locations of the PET transmission scan to the CT scan was then determined for x, y, z and total (vector) deviation for each of the four studies. These data yield an independent and objective measure of the goodness of the registration in the x, y and z directions as well as a value of the overall goodness of registration.

RESULTS

The results of the phantom study are summarized in Table 1 and Figure 2. In Table 1, the means and the standard errors of the mean of the rms deviations for the four PET transmission studies are listed. The rms deviations are also listed for the x, y, z and total (vector) deviations. In Figure 2, the total and z rms values along with the average z deviation are plotted versus the threshold value. The minimum z and total deviations correspond to when the average deviation in z is zero which occurs at a threshold value between 0.060 and 0.065. This corresponds to

TABLE 1
Root Mean Square Deviation (mm) as a Function of Threshold

Threshold	x	y	z	Total
0.040	2.24 ± 0.36	2.85 ± 0.60	9.53 ± 0.27	5.92 ± 0.28
0.050	1.86 ± 0.23	2.29 ± 0.49	5.66 ± 0.11	3.73 ± 0.10
0.055	2.22 ± 0.47	2.16 ± 0.38	4.55 ± 0.31	3.23 ± 0.27
0.060	1.80 ± 0.24	2.19 ± 0.42	2.77 ± 0.22	2.35 ± 0.15
0.065	1.80 ± 0.21	2.18 ± 0.36	3.03 ± 0.15	2.43 ± 0.13
0.070	2.17 ± 0.24	2.35 ± 0.28	5.76 ± 0.22	3.83 ± 0.13

For each of the four transmission studies, the locations of the nine markers were transformed by the matrix determined by the registration algorithm to generate a set of "registered" marker locations. The root mean square deviation between these registered locations and the locations of the markers for the CT scan were then determined as an objective measure of the goodness of fit. The x, y, z and total deviation were determined in each case. The values in the table represent the means and the standard errors of the mean for the four PET transmission studies. The z and total deviations are minimum for a threshold of 0.060, whereas threshold does not have a substantial effect on x and y deviations.
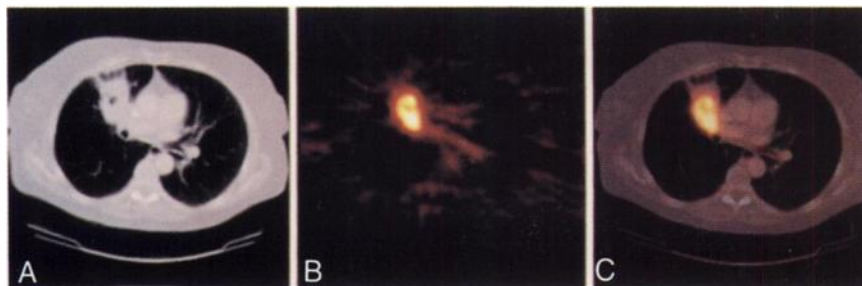
FIGURE 3. (A, B, C) CT, PET and merged images, respectively, from Patient 1.

approximately 50% of the maximum pixel value on the PET transmission scans. With a threshold value of 0.060, the rms deviations for x, y, z and the total are 1.80 mm, 2.19 mm, 2.77 mm and 2.35 mm, respectively.

The following three clinical cases demonstrate typical images for this technique and illustrate the utility and clinical significance of the combined display.

Patient 1

This patient, a 60-yr-old woman, had a known right lung mass. Figure 3A is a transverse CT slice through the thorax just below the carina. Figure 3B is a PET image that has been registered using the technique described above and sliced to match the CT image in Figure 3A. Figure 3C demonstrates the PET/CT merged image. With the CT image alone, it is difficult to distinguish the extent of tumor invasion into the mediastinum and chest wall. With the PET scan alone, the tumor is readily apparent but again it is difficult to determine, even with the CT image available for comparison, whether there is invasion into the mediastinum due to the lack of anatomical information in the PET scan. The combined image draws on the strengths of both modalities to aid in this difficult diagnosis. It is quite evident in viewing this image that the tumor does not invade the mediastinum, but it is intimately involved with the superior vena cava. The merged image also reveals the

density encroaching the chest wall in the CT image to more likely be a postobstructive pneumonia secondary to occlusion of the airway by the primary tumor.

Patient 2

This patient is a 74-yr-old woman with known squamous-cell carcinoma of the left lung and extensive infiltrative changes in both upper lungs. Figure 4A is a transverse CT slice through the thorax. Figure 4B is the registered and resliced PET image demonstrating uptake of FDG by the primary tumor site. In the CT image, there is a mass in the left posterior lung. Based on the CT images alone, it is difficult to determine if this is tumor, pneumonia, consolidation or scar tissue. Also, it is difficult to determine involvement of the chest wall based upon either the CT or PET studies alone. The combined image displayed in Figure 4C reveals the true extent of the active tumor within an area of consolidation and indicates likely chest wall involvement. Figure 4D is another transverse CT slice through the same patient at the level of the arch of the aorta. Extensive bilateral infiltrate is seen in this slice. The corresponding PET scan in Figure 4E reveals low-level uptake in the infiltrate consistent with a pneumonia rather than tumor. Figure 3F is the merged image displaying good correspondence between the area of probable pneumonia on the PET and the area of infiltrate on the CT.
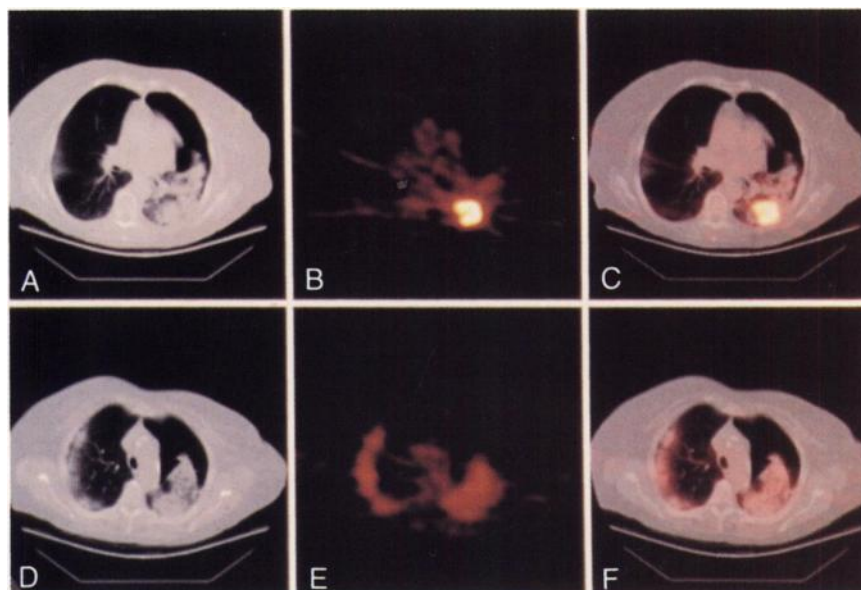

FIGURE 4. Two axial slices are shown. (A, D) CT scans, (B,E) PET scans and (C,F) merge images for the two slices, respectively.
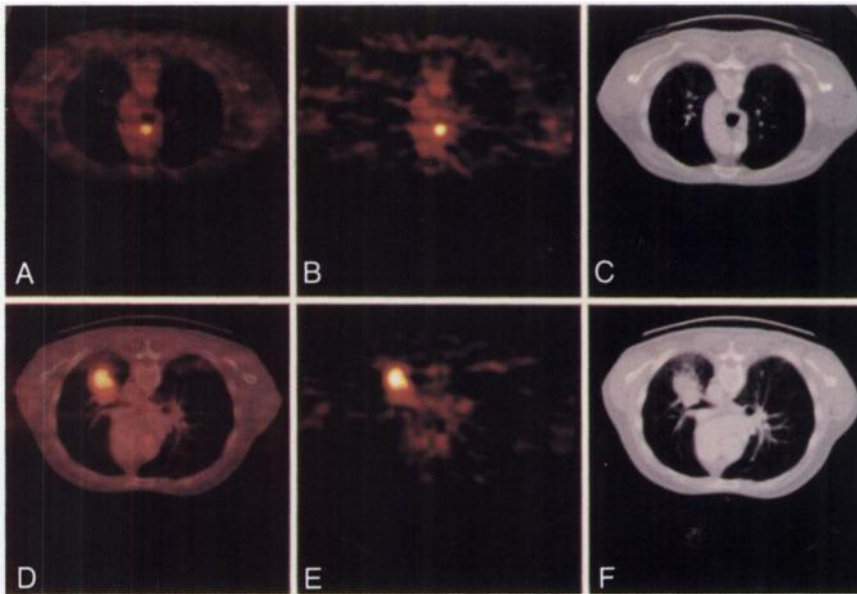
FIGURE 5. Two axial slices are shown. (A, D) CT scans. (B,E) PET scans and (C,F) are the merged images for the two slices, respectively.

Patient 3

This patient is a 51-yr-old man with a left lung mass suspected of being a bronchogenic carcinoma. Figure 5A shows a CT section at the level of the pulmonary hila. A mass is readily visible in this image. The corresponding PET emission image in Figure 5B demonstrates a region of increased FDG uptake in approximately the same region. The combined PET-CT image in Figure 5C demonstrates that only a portion of the mass shown in Figure 5A is likely to be an actively growing tumor. Another CT section from the same patient is shown in Figure 5D. No pathology is readily evident on this image. The corresponding PET image in Figure 5E demonstrates focal uptake of FDG consistent with nodal metastasis.

Looking at the PET study alone, however, it is difficult to determine the exact location of the metastatic node due to lack of anatomical information. Figure 5F makes exact localization of the metastatic node in a pretrachial location obvious.

DISCUSSION

We have developed an image segmentation technique which, in conjunction with the surface-fitting algorithm, yields an accurate registration of thoracic PET and CT. This technique, which involves the generation of surfaces from the chest wall, is potentially less susceptible to misregistration than methods using external fiducials since the pleura are in intimate contact with the thoracic cage. The rib cage is very reliable for surface definition since it is a relatively rigid structure and moves only minimally during quiet respiration. In addition, the large difference between the attenuation coefficients for soft and lung tissue make the pleural surface easily discernable.

The accuracy of this technique was evaluated by two basic approaches: quantitatively through a phantom study and by evaluation of the resulting clinical images. The

phantom study indicated that this technique was accurate to within 2–3 mm in all directions. Although the clinical examples in this report were acquired using a standard CT scanner (1 cm interslice spacing), the phantom data were obtained with a helical CT scanner. The phantom data were acquired in this manner because helical CT is the current modality of choice for these types of studies at our institution. Thus, the accuracy of the registration technique demonstrated by the phantom study is representative of our current, clinically applied method. It is expected that the accuracy of this technique with standard CT is slightly worse.

We evaluated the registration of the clinical images by several means. One method was to overlay the CT contours used in fitting onto the resliced PET transmission images. This overlay should align with the 50% isocontour in the resliced PET images. In all cases, the images appeared well aligned.

Another method of evaluation was to apply the dual-color scale merging procedure described in the Results section to the CT and resliced PET transmission study rather than the emission study. This method is more subjective than the contour overlay method just discussed, but it is useful because the two image sets are compared directly to each other rather than comparing a representation of an image set (a contour) to an image set.

Finally, the quality of the fit can also be evaluated by examination of the final images. Tumors seen on PET should overlay regions of density on CT. Similarly, areas of inflammation, consolidation or pulmonary collapse should be aligned between the two studies. We found that this was usually the case. We discovered, however, that features near the diaphragm were often displaced in the rostral-caudal axis relative to the same feature in the other modality. We associate this axial displacement with diaphragmatic motion during normal respiration. This motion is probably

accentuated because the CT images are obtained during breath holding while the PET images are obtained during tidal respiration. Since the majority of structures of interest are not near the diaphragm, particularly in tumor staging, we do not anticipate this to be a major problem.

It is important to have the PET scan and the CT scan be acquired within reasonable temporal proximity. Otherwise, it is possible to have anatomical changes in the time between the two scans that can render the registration inaccurate. For example, if a lobe collapses or pneumonia develops after the CT scan was acquired but prior to the PET scan, it will not be possible to accurately register the two studies.

An initial concern with the application of PET to the evaluation of lung carcinoma was that it would be difficult to discern tumor from such entities as consolidation or postobstructive pneumonia. Several of our studies, however, including those in this report, have indicated that the differences in these processes appear to be detectable.

Potential limitations of the intermodality registration method include:

1. Possible patient movement *between* the PET emission and transmission scans.
2. Possible patient movement *during* the PET emission or transmission or CT scans.
3. Positioning of the patient in the different scanners could also affect the intermodality display.
4. There is a known difficulty with diaphragmatic movement which has already been discussed.
5. The determination of the exact value to segment upon in both the CT and the PET transmission scan.

The limitations concerning patient motion and positioning are inherent in all registration techniques but do not appear to be serious. We are currently evaluating the misregistration between emission and transmission studies in PET through the use of a short transmission scan acquired postemission.

The concern unique to this protocol is the determination of the segmentation values for CT and PET. We need to determine values in both modalities that correspond to the pleural surfaces across multiple patients. Incorrect thresholds will lead to rostral-caudal mispositioning since we use the tapering of the lungs towards the apex as the determinant for the z-axis registration. Through our phantom study, we have arrived at threshold values for both the PET and CT images that lead to accurate registration.

CONCLUSION

Through a combination of techniques, a procedure has been developed that allows for accurate registration in the thorax. Image acquisition and conversion requires only minimal user intervention. Image segmentation has been automated so that it usually only takes 10 min and requires minimal training to define the pleural boundaries in both the PET transmission and CT studies. We had initially performed the segmentation by hand. By defining the ap-

propriate window and level values, one could generally define the pleural boundaries, but the definition of the most anterior and posterior aspects of the contours was problematic. Thus, automatic segmentation was determined to be an essential aspect of the method. The remainder of the registration, including contour generation, contour fitting, image reslicing and image merging, require only minimal user intervention and take approximately 35 min on a Sun Sparc 2.

This procedure will continue to be refined and a study will be performed to compare the diagnostic accuracy of the results to those obtained from CT alone, PET alone and PET in combination with CT. These results will be compared to surgical exploration and biopsy with pathological evaluation as the gold standard. Further improvements in the merged or combined display are also needed and are under investigation.

ACKNOWLEDGMENTS

REFERENCES

1. Schelbert HR. Positron emission tomography for the assessment of myocardial viability. *Circulation* 1991;84(suppl I):I122–I131.
2. Gupta NC, Frank AR, Dewan NA et al. Solitary pulmonary nodules: detection of malignancy with PET with 2-[F-18]-fluoro-2-deoxy-D-glucose. *Radiology* 1992;184:441–444.
3. Alpert NM, Bradshaw JF, Kennedy D, Correia JA. The principle axes transformation—a method for image registration. *J Nucl Med* 1990;31:1717–1722.
4. Wilson MW, Mountz JM. A reference system for neuroanatomical localization on functional reconstructed cerebral images. *J Comput Assist Tomogr* 1989;13:174–178.
5. Pietrzyk U, Herholz K, Heiss W-D. Three-dimensional alignment of functional and morphological tomograms. *J Comput Assist Tomogr* 1990;14:51–59.
6. Pelizzari CA, Chen GTY, Spelbring DR, Weichselbaum RR, Chen C-T. Accurate three-dimensional registration of CT, PET and MR images of the brain. *J Comput Assist Tomogr* 1989;13:20–26.
7. Levin DN, Pelizzari CA, Chen GTY, Chen C-T, Copper MD. Retrospective geometric correlation of MR, CT, and PET images. *Radiology* 1988;169:817–823.
8. Turkington TG, Jaszczak RJ, Pelizzari CA et al. Accuracy of registration of PET, SPECT and MR images of a brain phantom. *J Nucl Med* 1993;34:1587–1594.
9. Bettinardi V, Gilardi MC, Lucignani G, et al. Procedure for patient repositioning and compensation for misalignment between transmission and emission data in PET heart studies. *J Nucl Med* 1993;34:137–142.
10. Bacharach SL, Douglas MA, Carson RE, et al. Three-dimensional registration of cardiac positron emission tomography attenuation scans. *J Nucl Med* 1993;34:311–321.
11. Kramer EL, Noz ME, Sanger JJ, Megibow AJ, Maguire GQ. CT-SPECT fusion to correlate radiolabled monoclonal antibody uptake with abdominal CT findings. *Radiology* 1989;172:861–865.
12. Wahl RL, Quint LE, Cieslak RD, Aisen AM, Koeppe RA, Meyer CR. "Anatometabolic" tumor imaging: fusion of FDG-PET with CT or MRI to localize foci of increased activity. *J Nucl Med* 1993;34:1190–1197.
13. Yu JN, Fahey FH, Harkness BA, Gage HD, Eades CG, Keyes JW Jr. Evaluation of emission-transmission registration in thoracic PET. *J Nucl Med* 1994;35:1777–1780.